frontiers | Frontiers in Earth Science

ORIGINAL RESEARCH
published: 25 April 2022
doi: 10.3389/feart.2022.889302

Mechanism and Controlling Factors on Methane Yields Catalytically Generated From Low-Mature Source Rocks at Low Temperatures (60–140°C) in Laboratory and Sedimentary Basins

Lin Wei[1,2]*, *Jia Yin*[1,2], *Jiansheng Li*[1,2], *Kun Zhang*[3]*, *Chunzhen Li*[1,2] and *Xiong Cheng*[1,2]

[1]School of Energy Resources, China University of Geosciences, Beijing, China, [2]Key Laboratory of Marine Reservoir Evolution and Hydrocarbon Enrichment Mechanism, Ministry of Education, Beijing, China, [3]School of Geosciences and Technology, Southwest Petroleum University, Chengdu, China

OPEN ACCESS

Edited by:
Shu Jiang,
The University of Utah, United States

Reviewed by:
Wei Yang,
China University of Petroleum, Beijing, China
Liangwei Xu,
Peking University, China
Siding Jin,
Chengdu University of Technology, China

***Correspondence:**
Lin Wei
linwei@cugb.edu.cn
Kun Zhang
201999010133@swpu.edu.cn

Specialty section:
This article was submitted to Geochemistry, a section of the journal Frontiers in Earth Science

Received: 04 March 2022
Accepted: 25 March 2022
Published: 25 April 2022

Citation:
Wei L, Yin J, Li J, Zhang K, Li C and Cheng X (2022) Mechanism and Controlling Factors on Methane Yields Catalytically Generated From Low-Mature Source Rocks at Low Temperatures (60–140°C) in Laboratory and Sedimentary Basins. Front. Earth Sci. 10:889302. doi: 10.3389/feart.2022.889302

Various studies have shown that geo-catalytically mediated methanogenesis could happen in immature to early-mature source rocks at temperatures ranging from 60 to 140°C based on a series of long-term laboratory heating experimental evidences. The results of those studies show that methane yields at the given temperature are 5–11 orders of magnitude higher than the theoretically predicted yields from early thermogenic methane generation kinetic models. However, different types of source rocks in these laboratory simulation experiments generated varied CH_4 and CO_2 yields, which suggest that controls on CH_4 generation during catalytic methanogenesis are complex. This study summarizes and compares gas yield results from laboratory low-temperature heating simulation experiments. Pre-existing trapped methane in rock chips could mimic newly generated gas during heating. The yields of catalytically generated CH_4 from individual source rocks were re-quantified by subtracting the amounts of pre-existing CH_4 in the closed pores of the original source rocks from the total methane amounts released from heating experiments and pre-existing CH_4 in the closed pores in heated source rocks. The results show that heating temperature and time exert a positive influence on methane catalytic methanogenesis. Mowry and Second White Specks Formation Shale generated approximately ten times more CH_4 than New Albany Shale and Mahogany Shale per gram of total organic carbon (TOC). Samples of Springfield Coal #1 and #2 exhibited ten times yield difference from one another at the same heating temperature. Those yield differences are not strongly associated with TOC content, heating time, temperature, metal content, or kerogen type but appear to be more influenced by maceral composition and also maceral–mineral contact area within the source rocks. We conclude that macerals in the liptinite group have a propensity for methanogenesis. Specifically, amorphous organic matter undergoes transformation into hydrocarbons earlier than alginite at low-temperature heating conditions. Sporinite also contributes to higher yields of methane released from the coal source rock. Vitrinite and inertinite show a positive influence on

carbon dioxide but no significant effect on increasing methane yields compared to other macerals. The strongest catalytic methanogenesis in the studied sample produced methane yields at 60°C, which amounted to ~2.5 μmol per gram of organic carbon during one year of heating. We suggest that geocatalytic methanogenesis could generate economically sizeable gas plays from immature to early-mature source rocks over geologic time.

Keywords: methane, source rock, low-mature, catalytic gas, maceral

1 INTRODUCTION

Hydrocarbon gases in source rocks in sedimentary basins are generally of either low-temperature microbial or high-temperature thermogenic origin (Tissot and Welte, 1984; Hunt, 1996; Whiticar, 1999; Paull et al., 2000; Jarvie et al., 2007; Martini et al., 2008). Microbial gas generation usually occurs in low maturity rocks when vitrinite reflectance (R_o) is lower than 0.4% up to 75°C (Rice and Claypool, 1981; Inagaki et al., 2015; Milkov and Etiope, 2018). Thermogenic gas generation resulting from kerogen and oil cracking typically falls into the R_o ranges of 0.8–1.3% (Higgs, 1986; Jarvie et al., 2007). However, numerous studies reported economically viable natural gas plays sourced from low-maturity coals and shales with R_o of 0.3–0.7% (e.g., Galimov, 1988; Xu et al., 2008; Cardott, 2012). The reported carbon and hydrogen isotopic values of methane gas ($\delta^{13}C_{CH4}$ from ~−55 to −30‰) from those gas occurrences were placed between typical microbial and thermogenic methane gas ranges, which made it difficult to determine their origins (Galimov, 1988; Muscio et al., 1994; Rowe and Muehlenbachs, 1999; Tilley and Muehlenbachs, 2006; Cardott, 2012). Researchers have made arguments about whether those natural gases are a mixture of thermogenic gas and microbial gas or those are gases migrated from deeper, thermogenic sources. In addition, as early as the 1980s, some researchers proposed that immature source rock could generate hydrocarbon gas catalytically at low-temperature conditions. The proposed hypotheses are as follows: 1) reduced metallic catalyst aids in the conversion of kerogen, bitumen, and oil to hydrocarbon gas (Mango, 1992; Lewan et al., 2008); 2) clay minerals facilitate the generation of hydrocarbons from organic matter (Espitalié et al., 1984; Bu et al., 2017; Rahman et al., 2018), although some other studies show that smectite inhibits hydrocarbon generation (Orr, 1983; Lewan and Kotarba, 2014) and montmorillonite can exhibit either pyrolysis-promoting or pyrolysis-inhibiting effect based on interlayer of clay-organic matter complexes (Bu et al., 2017); 3) sulfur-bearing kerogen with low activation energy for hydrocarbon generation (Baskin and Peters, 1992; Lewan, 1998; Seewald, 2003); and 4) certain types of macerals undergo easier and earlier bond breaking to generate light hydrocarbons (Peters et al., 2006; Liu et al., 2019a).

Long term low-temperature (<200°C) simulation experiments in laboratory conditions can simulate the natural hydrocarbon gas generation process in sedimentary basins. Unlikely traditional hydrous pyrolysis experiments (<350°C; Lewan, 1991; Savage, 2000; Kotarba and Lewan, 2004; Stainforth, 2009), low temperature create proper conditions for metallic catalyst activation and for macerals to reach their initial activation energy-generating hydrocarbons gradually (Mango, 1992; Medina et al., 2000; Lewan et al., 2008). In recent years, our research group conducted a series of low-temperature (60–140°C) and long term (1 month–5 years) heating experiments to investigate an alternative, low-temperature pathway for C–C bond breaking and the generation of non-microbial coalbed gas and shale gas. Several different source rocks in these simulation experiments generated varied amounts of CH_4 and CO_2, and also carbon and hydrogen isotopic values of methane (Wei et al., 2018; Wei et al., 2019; Ma et al., 2021). The results of Wei et al. (2018) show that methane yields in New Albany Shale (NAS) at the given temperature are 5–11 orders of magnitude higher than the theoretically predicted yields from kinetic models of early thermogenic methane generation. Those studies proved that both shale and coal could be geo-catalytically converted into gaseous hydrocarbons at temperatures as low as 60°C, and ~200°C could be the start temperature for thermal cracking of OM. For thermogenic gases, their generation yields are strongly correlated with total organic carbon (TOC) content, kerogen type and initial maturity (Jarvie et al., 2007; Gao et al., 2014; Lewan and Kotarba, 2014; Wei et al., 2016; Wei et al., 2021). Previous studies (Wei et al., 2018; Wei et al., 2019) indicated that increased temperature and heating time enhanced catalytic methane yields, while elevated pressure exerted a negative influence on catalytic methane generation However, when yields from many different source rocks were compared at a similar temperature, heating time, and pressure conditions, it was difficult to generalize the major factors controlling CH_4 generation during catalytic methanogenesis. For example, Mowry and Second White Specks Formation Shale generated approximately ten times more CH_4 than New Albany Shale and Mahogany Shale per gram of TOC. Samples of Springfield Coal #1 and #2 exhibit ten times yield difference at the same heating temperature.

Organic matter is the material basis for hydrocarbon transformation and generation. Macerals can have variable hydrocarbon generation potential within the source rock. Individual macerals evolve differently along with maturation and could be oil-prone, gas-prone, or could have very limited hydrocarbon generation potential (Peters et al., 2006; Mastalerz et al., 2012; Mastalerz et al., 2018; Wei et al., 2016; Liu et al., 2019a). For example, the liptinite maceral group includes oil-prone macerals such as alginite, cutinite, sporinite, and amorphous organic matter (AOM; also named bituminite or

amorphinite; ICCP, 1998; ICCP, 2001). Same geochemically-defined kerogen types could have heterogeneous maceral composition (ICCP, 1998; ICCP, 2001; Taylor et al., 1998; Mastalerz et al., 2012; Hackley and Cardott, 2016; Pickel et al., 2017; Liu et al., 2019a; Liu et al., 2019b; Liu et al., 2020). More specifically, type III kerogen might be composed dominantly of gas-prone vitrinite macerals or might be a mixture of type II and IV and thus have significant oil-prone character. For example, the coals and the dispersed organic matter in Cooper Basin are composed of large content of inertinite but several percent of degraded alginite, which has been widely regarded as a source of oil (Smyth, 1983; Taylor et al., 1998; Jadoon et al., 2016). In addition, the source rock's onset to generate hydrocarbons varies depending on the specific maceral type and association (Khorasani and Murchison, 1988; Snowdon, 1991; Lin and Ritz, 1993; Yang et al., 2017), while their conclusions differ from each other. Some researchers proposed that the immature oil mainly originated from resinite (Khorasani and Murchison, 1988; Snowdon, 1991), and most of the other liptinitic maceral begin to generate oil earlier than alginite (Khorasani and Murchison, 1988). Other studies indicated that amorphous liptinite generated oil earlier than other macerals (Khorasani and Michelsen, 1991; Liu et al., 2017). Lin and Ritz (1993) concluded that vitrinite and resinite are more branched aliphatic chains which can reduce the bond dissociation energies of kerogen (Lin and Ritz, 1993). However, most of the research that addressed differences in hydrocarbon generation for individual macerals focused on maceral generation ability during thermal cracking at high-temperature conditions (>200°C), whereas their gas generation potential at low-temperature conditions remains unclear.

This article summarized gas product yields from a variety of source rocks from laboratory low-temperature heating simulation experiments of our research group performed over the last several years (Wei et al., 2018; Wei et al., 2019; Ma et al., 2021). Geochemical and petrographic differences, especially the maceral characterization under a microscope between source rock samples, were further investigated and compared. Natural gas geochemical data reported from other sedimentary basins are also provided for comparison. A previous study suggested that the low-temperature regime of catalytic methanogenesis entailed a low but continuous gas generation rate. For example, at the measured sustained rate, the entire supply of TOC in Mowry Shale could be converted to methane over a period of 25,000 years (Wei et al., 2018). However, in reality, when oil-prone maceral transformation begins, bitumen and oil become the main reaction product, which makes the whole process of conversion and generation rate estimation more complex. Nevertheless, controlling factors, especially the influence of maceral type and its transformation on the gas generation yield, remain a critical problem for evaluating the gas play potential in sedimentary basins and low-maturity basins in particular.

2 MATERIALS AND METHODS

2.1 Source Rocks

This study used thermally immature to early mature shales and coals with R_o values from 0.39 to 0.62%. Samples from various basins have different TOC contents, ages, and kerogen types of I, II, and III (**Table 1**). Samples were crushed into chips (size range from 1 to 5 mm) or powders (0.25–0.42 mm) for use in our experiments (**Table 2**). Samples sealed in rigid glass tubes were heated at ambient pressures. All rock chips were placed under vacuum at room temperature for 2 days to remove volatile hydrocarbons prior to heating experiments. Heating from 60°C to 140°C tested gas generation at temperatures similar to those typically encountered in sedimentary basins (**Table 2**).

2.2 Extended Heating Experiments

2.2.1 Heating for 1 Month in Glass Tubes

Two types of source rock (listed in **Tables 1**, **2**), Yabulai Shale and New Albany Shale $(NAS)_{472\text{-}RD,}$ were crushed and sieved to sizes of 40–60 mesh (250–420 μm). Samples were evacuated for 3 days at either 100°C (for samples designated for later heating at 100°C) or at 140°C (for samples slated for heating above 100°C) to remove pre-existing adsorbed gas.

2.2.2 Heating for 12–38 Months in Glass at Low Pressure

Six different types of source rocks (**Table 2**), i.e., Mowry Shale, Mahogany Shale, $NAS_{472\text{-}RD}$, NAS_{MM3}, Wilcox Lignite, and Springfield Coal #1, were crushed and sieved to 1–3 mm chip size. Experimental conditions were 60 and 100°C heating for 12 months at ambient pressures. Four types of source rock, i.e., NAS_{IN3}, NAS_{IN6}, Second White Specks Formation, and Springfield Coal #2 (**Table 2**), were crushed and sieved to chips with sizes 1–5 mm diameter.

Aliquots of all dry chips were weighed and loaded into pre-annealed, ~9-mm o.d. Pyrex glass ampoules. Each ampoule received a constriction near its top to later facilitate sealing under vacuum and then received 0.2 ml of deionized water from a syringe. After flushing the headspace with argon to remove air, each glass ampoule was hermetically sealed using argon arc welding. The glass ampoules/gold cells were placed into a vacuum chamber for 11 h. Those ampoules were also weighed before and after vacuum-dried to check for leaks. The sealed ampoules were autoclaved at 121°C for 30 min to exclude the activity of methanogenic microbes.

Glass ampoules were immersed into heated glycerol baths or ovens that were kept isothermal at either 60, 80, 100, 120, or 140°C for periods between 1, 12, 14, 36, and 38 months (**Table 2**).

Sets of duplicate samples were used to evaluate reproducibility. Heating experiments of these duplicate samples were performed using equivalent time, pressure, and temperature conditions to evaluate the overall reproducibility of the methane yield.

2.3 Collection and Quantitation of Gas Products

All generated gas products from glass ampoules were collected using the same glass vacuum line (**Figure 1**) by following the principles outlined by Wei et al. (2018). After opening the glass ampoule and releasing product gases into the vacuum line, the condensable gas fraction (predominantly CO_2) and the incondensable gas fraction (including hydrocarbon gas and nitrogen gas) were separately collected. The Baratron readings

TABLE 1 | Low-maturity source rock starting materials: kerogen type, total organic carbon (TOC) content, maturity (expressed by vitrinite reflectance R_o), age, and geographic origin. The pH values were measured in water in contact with the powdered original rock.

Rock unit name	Kerogen type	TOC content (wt.%)	R_o (%)	Age	Origin	pH
New Albany Shale $NAS_{472\text{-}RD}$	II	1.2	0.42	Devonian	Indiana	n.d.
New Albany Shale NAS_{IN3}	II	5.6	0.54	Upper Devonian	Daviess Co., Indiana	7.7
New Albany Shale NAS_{IN6}	II	15.1	0.51	Upper Devonian	Harrison Co., Indiana	8.1
Yabulai Shale	II	5.2	0.47	Jurassic	Inner Mongolica, China	n.d.
Second White Specks Formation Shale	II	3.8	0.42	Cretaceous (Cenomanian)	Alberta, Canada	7.9
Mowry Shale	II	2.5	0.57	Cretaceous	Colorado	8.1
Springeild Coal #1	III	69	0.54	Pennsylvanian	Indiana	4.4
Springfield Coal #2	III	69	0.54	Pennsylvanian	Gibson Co., Indiana	4.7
Wilcox Lignite	III	58	0.39	Paleocene	Texas, United States	n.d.
NAS_{MM3}	II	5.8	0.62	Devonian	Indiana	6.9

TABLE 2 | Characterization of experimental heating conditions with regard to source rock type, chip diameter, temperature, and heating duration.

Sets of experiments	Chip diameter (mm)	Heating temperature (°C)	Heating duration (months)
Mowry Shale	1 to 3	60 and 100	12
Mahogany Shale	1 to 3	60 and 100	12
$NAS_{472\text{-}1\text{-}RD}$	1 to 3	60 and 100	12
NAS_{MM3}	1 to 3	60 and 100	12
Wilcox Lignite	1 to 3	60 and 100	12
Springfield Coal #1	1 to 3	60 and 100	12
NAS_{IN3}	1 to 5	80, 100, and 120	36
NAS_{IN6}	1 to 3	80 and 100	14
Second White Specks Formation	1 to 3	80 and 100	38
Springfield Coal #2	1 to 5	80, 100, and 120	36
$NAS_{472\text{-}1\text{-}RD}$	0.25 to 0.42	100 and 140	1
Yabulai Shale	0.25 to 0.42	100 and 140	1

from injected known volumes of pure CH_4 or CO_2 were used to calibrate pressure responses in distinct partial volumes of the vacuum line (not only to calculate gas yields in μmol but also to determine volume split ratios; **Figure 1A**). All gases were finally transferred to a methane receptacle with charcoal, followed by sealing off with a torch. The resulting sealed gas sample was transferred into a 10 ml/60 ml Pyrex® culture glass bottle and subsequently crimp-sealed.

Wei et al. (2018, 2019) quantified generated gas products with an SRI Multiple Gas Analyzer #2 (Jin et al., 2010) based on gas chromatography, using a flame ionization detector (FID) to detect C_1–C_4 hydrocarbon gases and a thermal conductivity detector (TCD) to quantify H_2, O_2, N_2, CH_4, CO, and CO_2 (**Figure 1A**). The GC column oven was initially held at 40°C for 4 min, followed by an increase to 250°C at 30°C min^{-1}, where it was held isothermally for 19 min. The GC precision for standard gases was better than ±400 ppmv for CO_2, ±10 ppmv for CH_4, and ±4 ppmv for C_2H_6 and C_3H_8.

Ma et al. (2021) quantified generated gas product with a SARAD RTM2200 gas analyzer (SARAD GmbH, Dresden, Germany), equipping 1) a madur madIR-D01 CO_2 detector (madur electronics, Zgierz, Poland, www.madur.com) and 2) an Axetris laser OEM module LGC F200 (Axetris AG, Kägiswil, Switzerland) to quantify CH_4. A detailed analyzing procedure is described by Ma et al. (2021). The system was calibrated by injecting known volumes of pure CH_4 or CO_2 with a gas-tight syringe through polymer tubing. The overall CH_4 and CO_2 yields from headspaces in glass tubes were calculated by taking into account the known gas split ratios between small and large gas fractions that had been separated at the vacuum line (**Figure 1B**).

2.4 Corrections on the Yields of Gas Product

The liberation of pre-existing trapped methane from source rock chips during heating and fracturing of rock through heating and subsequently mimicking catalytically generated gas. The most commonly used method to evaluate residual gas in source rocks is by crushing in a closed environment, such as a ball mill chamber. Wei et al. (2018) assessed methane volumes released from shales and coals by crushing chips in a modified 65–mL SPEX 8000 ball mill (operated at 1080 cycles per minute) using a SPEX 8001 Hardened Steel Grinding Vial Set (http://www.spexsampleprep.com/equipment-and-accessories/accessory_product/8001) that had been fitted with a septum port to obtain gas samples from the closed mill chamber using a gas-tight syringe (**Figure 1A**). Pairs of 12.7- and 6.4-mm diameter alloy steel 52–100 crushing balls contained Fe, Cr, Mn, and 0.98–1.1 wt. % of C in the form of metal carbides in steel (http://www.suppliersonline.com/propertypages/52100.asp). Wei et al. (2018) demonstrated that adding deionized water to the ball mill and crush with samples together is effective for reducing the localized heating when the kinetic energy of a steel ball is converted into heat upon impact. Aliquots of 1 g of chips were loaded into the

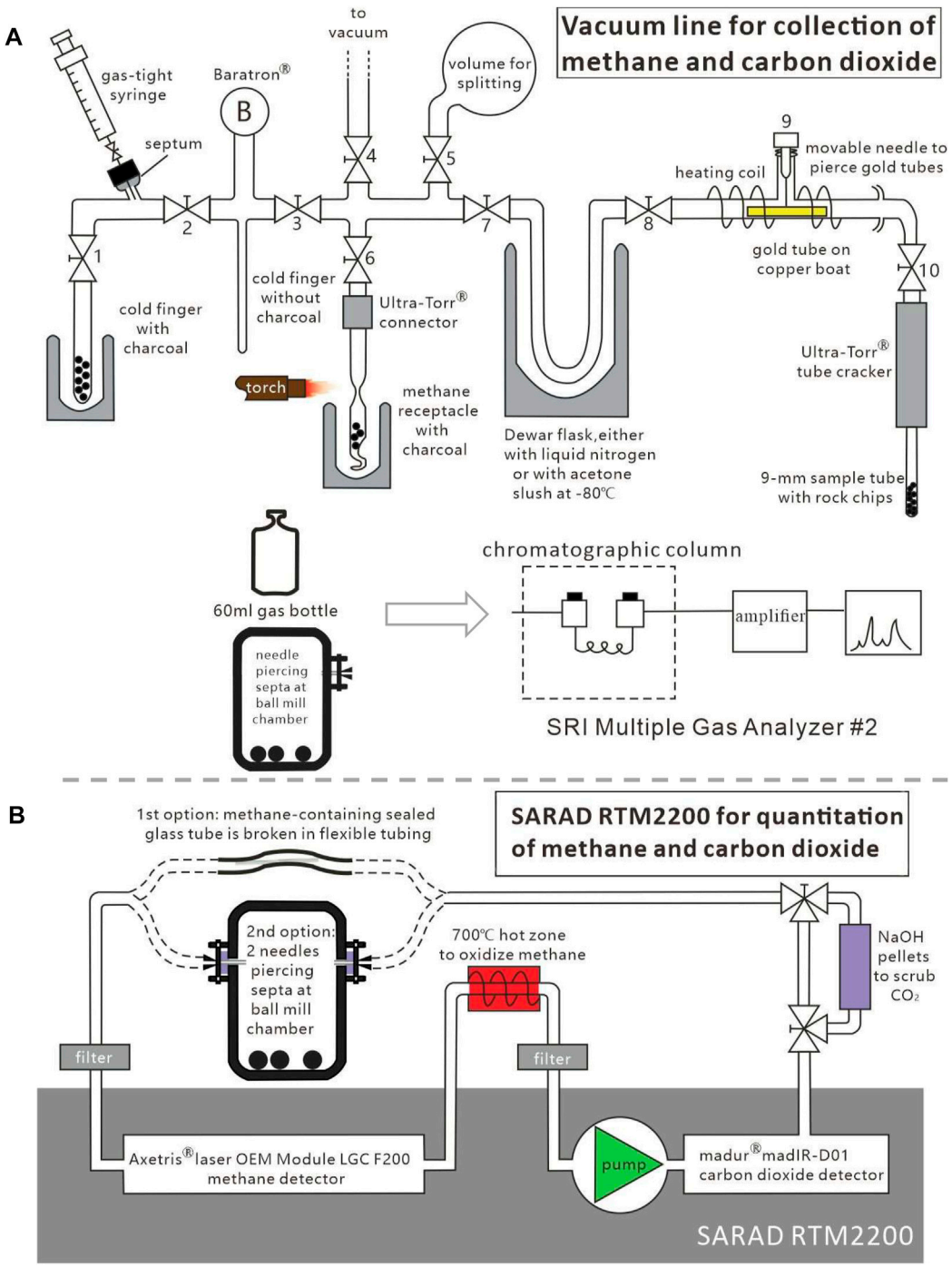

FIGURE 1 | Schematic diagram showing gas collection process. **(A)** Glass vacuum line for cryogenic collection of gases from glass ampoules after low-temperature heating experiments (modified from Wei et al., 2018). Collected methane/carbon dioxide gas in the receptacle under valve 6 and gas released from 65–mL SPEX 8000 ball mill were separately transferred using a syringe to SRI multiple gas analyzer for quantification **(B)** Schematic diagram of quantitation of CH_4 and CO_2 with a SARAD RTM2200 gas detector system with closed-circuit gas flow (modified from Ma et al., 2021).

ball mill with an addition of 0.4 ml deionized water, the headspace was flushed with ultra-high purity nitrogen, and milling proceeded for 4 min, followed by methane quantification in headspace gas *via* GC. Wei et al. (2018) used gas-tight syringes to transfer gas aliquots from a ball mill chamber with a single septum port to a gas chromatograph to quantify CH_4 yields from source rocks after ball milling. They reported varied amounts of pre-existing gases in closed pores of original, un-heated source rocks. For example, Mowry

Shale has 0.013 and 2.059 μmol g^{-1} pre-existing CH_4 and CO_2 in rock chips before heating. They also further quantified the amount of gas released from the gas ampoules and the amount of gas in closed pores from heated source rocks under different heating conditions in the study.

Wei et al. (2019) pre-evacuated Yabulai Shale and $NAS_{472\text{-}RD}$ for 3 days before long-term heating simulation experiments. Those samples were at 60 mesh (0.25–0.42 mm) and were proposed to have removed pre-existing adsorbed gas. Gas yields from those experiments did not require further correction.

Ma et al. (2021) made further efforts in ball milling and gas detection with a highly sensitive SARAD RTM2200 system that did not require any gas transfer using a syringe. They provided new evidence for a largely systematic, non-negligible contribution of pre-existing CH_4 from imperfectly closed pores. They used the source rock–specific average deficits of gases between original and heated source rocks to correct the overall gas yields. Their study concluded that the gas content in closed pores was fixed for each series of samples and used the results from the ball milling experiments to determine the average amounts of CH_4 [and CO_2] that had leaked from imperfectly closed pores. Their reported data were presented as corrected yield and uncorrected yield. The final corrected methane yields were uncorrected yields subtracting certain amounts. For each one of the four source rocks used (i.e., Springfield Coal #2, NAS_{IN3}, NAS_{IN6}, Second White Specks Fm.), the respective subtracting amounts in μmol g^{-1} TOC are 0.05 [4.19], 0.06 [3.04], 0.02 [8.11], and 0.40 [8.96] (CH_4 yield [CO_2 yield]).

To make a better gas generation yield comparison between different studies (Wei et al., 2018; Ma et al., 2021), the amount of newly generated gas in each study is re-calculated by subtracting yields of residual gas in closed pores of original, un-heated samples from total yields of released gas from glass ampoules and residual gas in closed pores from source rock chips after heating experiments. Powdered samples of 60-mesh heated for 1 month (Wei et al., 2019) had removed pre-existing gas and could avoid the calculation above.

2.5 Analysis of Metal Concentrations

Metal concentrations were obtained using a method modified from the one used by Kendall et al. (2009). An aliquot of 40–50 mg of powdered, whole-rock shale was baked for 12 h in a 550°C oven. The ashed powder was then treated with 5 ml of HNO_3 and 1 ml of concentrated hydrofluoric acid (HF) and placed on a 200°C hot plate for 10 h. Due to moderated organic content in samples, repeated HNO3-HF treatment was performed to fully dissolve the organic matter. Samples were dried and treated with HCl after dissolution and were diluted with HNO_3. Metal abundances were measured by inductively coupled plasma-mass spectrometry (ICP-MS) against multiple-element calibration standards. Analyte concentration reproducibility was better than 5%.

3 RESULT AND DISCUSSION

3.1 Methane and Carbon Dioxide Gas Released From Closed Pores

Researchers have proposed and proved the existence of catalytic gas generation eluding biogenic gas contribution using in-lab low-temperature long time heating simulation experiments in recent years (Carothers and Kharaka, 1978; Mango, 1996; Rowe and Muehlenbachs, 1999; Tilley and Muehlenbachs, 2006; Xu et al., 2008; Mango and Jarvie, 2009; Wei et al., 2018; Wei et al., 2019; Ma et al., 2021). Wei et al. (2018, 2019) used different coal and shale samples and generated CH_4 and CO_2 gas from 60°C to 140°C based on a series of 1–24 months of heating experiments. Ma et al. (2021) adjusted and improved the gas yield measurement method with additional source rock samples using similar heating experiments. However, pre-existing trapped methane may become liberated during heating and fracturing of rock at high pressure and subsequently mimic catalytically generated gas. Extended evacuation of rocks chips before heating experiment at room temperature cannot remove all pre-existing gas trapped in closed pores. Previous studies reported three types of methane amount, i.e., the amounts of pre-existing gases in closed pores of original (before the heating experiment), un-heated source rocks, the amounts of gases in closed pores of heated source rocks (after the heating experiment), and the amounts of gases released from gas ampoules (after the heating experiment).

The yield of methane from Mowry Shale in Wei et al. (2018)'s experiment is much lower compared to that in the research conducted by Mango and Jarvie (2009) using a short-term heating experiment. Mango and Jarvie (2009) heated Mowry Shale (60-mesh) to 100°C for 24 min in a flow-through reactor. The helium effluent carried a cumulative yield of 25 μg g^{-1} C_1–C_5 hydrocarbons claimed to be of catalytic origin. Using the same heating apparatus at 50°C with Floyd Shale, Mango and Jarvie (2009) observed a chaotic pattern of distinct methane pulses eluting over time that was interpreted as a characteristic hallmark of catalysis. We concluded that no single microscopic catalytic domain in shale can spontaneously generate enough methane to emit a gas pulse that is detectable with a GC. A more likely explanation for the observed methane pulses from Mowry Shale is the developing mechanical stress within Mowry Shale during exposure to ultrapure helium. The diffusive influx of helium through narrow throats into pores containing pre-existing methane causes pore overpressure.

The method used to evaluate residual gas in source rocks is by crushing in a closed environment, such as a ball mill chamber. Water was present in the ball milling experiments as a coolant to limit the thermal stress during steel ball impacts. Wei et al. (2018) first claimed that dry ball milling experiments greatly introduced inorganic methane from metal carbides from the steel surface of the ball mill chamber, and moist ball milling experiments collected methane yields of 0.021 μmol g^{-1} can be accounted for by a reaction of metal carbides. Ma et al. (2021) proposed that the absence of any additional solid substrate did not prevent abrasion as steel balls impacted the steel walls and generated 0.05 μmol g^{-1} CH_4 and 0.24 μmol g^{-1} CO_2. The differences could be accounted to the cleanness of rock powder attached to the ball mill chamber between runs, the gas collection and transfer process between different runs, and the sensitivity between the SARAD RTM2200 system and traditional gas chromatography. Although varied quantification of pre-existing gas amount exists between the two studies, the real catalytic gas generation amount

TABLE 3 | Yields of methane and CO_2 generated catalytically at 60, 80, 100, 120, and 140°C after months of heating experiments.

Sample name	TOC (wt. %)	Heating temp. (°C)	Heating duration (months)	Catalytic CH_4 yield (μmol g^{-1} TOC)	Catalytic CO_2 yield (μmol g^{-1} TOC)
NAS_{IN3}, 80°C	5.6	80	36	0.3	253
Al foil					
Al foil	5.6	80	36	n.d.	149
	5.6	80	36	0.3	362
	5.6	80	36	0.1	283
	5.6	80	36	0.3	245
	5.6	80	36	0.2	247
$NAS_{472\text{-}D}$, 100°C	1.2	100	12	1.12	n.d.
NAS_{MM3}, 60°C	5.8	60	12	0.31	450.2
NAS_{MM3}, 100°C	5.8	100	12	0.58	455.6
NAS_{IN3}, 100°C	5.6	100	36	0.28	1061
	5.6	100	36	0.63	1106
	5.6	100	36	0.28	1158
	5.6	100	36	0.68	1510
NAS_{IN3}, 120°C	5.6	120	36	0.22	563
	5.6	120	36	0.42	321
	5.6	120	36	0.43	668
	5.6	120	36	0.29	433
	5.6	120	36	0.45	313
	5.6	120	36	0.32	339
	5.6	120	36	0.37	293
	5.6	120	36	0.46	298
NAS_{IN6}, 80°C	15.1	80	14	0.29	162
	15.1	80	14	0.11	179
	15.1	80	14	0.13	200
	15.1	80	14	0.16	209
	15.1	80	14	0.13	196
	15.1	80	14	0.08	204
	15.1	80	14	0.13	186
NAS_{IN6}, 100°C	15.1	100	14	0.23	399
	15.1	100	14	0.19	453
	15.1	100	14	0.21	379
	15.1	100	14	0.21	388
	15.1	100	14	0.27	370
	15.1	100	14	0.22	334
Springfield Coal #2, 80°C	69.0	80	36	3.41	1.4
	69.0	80	36	3.25	2.8
	69.0	80	36	2.10	2.6
	69.0	80	36	3.17	1.0
Al foil	69.0	80	36	3.26	2.4
Springfield Coal #2, 100°C	69.0	100	36	2.77	2.0
	69.0	100	36	2.61	0.4
	69.0	100	36	2.66	1.9
	69.0	100	36	2.24	7.1
Springfield Coal #2, 120°C	69.0	120	36	3.42	2.5
	69.0	120	36	2.73	4.2
	69.0	120	36	3.95	5.7
	69.0	120	36	2.45	3.8
Springfield Coal #1, 60 °C	69.0	60	12	0.13	26.5
	69.0	60	12	0.13	25.6
Springfield Coal #1, 100°C	69.0	100	12	0.26	32.2
Second White Specks Formation 80°C	3.8	80	38	2.55	534
	3.8	80	38	2.16	617
	3.8	80	38	3.00	395
	3.8	80	38	2.35	494
	3.8	80	38	2.55	588
	3.8	80	38	2.41	501
Second White Specks Formation 100°C	3.8	100	38	5.05	3224
	3.8	100	38	5.49	4133
	3.8	100	38	4.47	3153
	3.8	100	38	5.49	3750
	3.8	100	38	4.92	2930
	3.8	100	38	5.39	3139

(Continued on following page)

TABLE 3 | (*Continued*) Yields of methane and CO_2 generated catalytically at 60, 80, 100, 120, and 140°C after months of heating experiments.

Sample name	TOC (wt. %)	Heating temp. (°C)	Heating duration (months)	Catalytic CH_4 yield (μmol g^{-1} TOC)	Catalytic CO_2 yield (μmol g^{-1} TOC)
Mowry Shale 60°C	2.5	60	12	2.78	188.4
	2.5	60	12	2.35	190.4
	2.5	60	12	2.63	192.3
Mowry Shale 100°C	2.5	100	12	5.21	354.2
	2.5	100	12	4.99	345.1
Mahogany Shale 60°C	15.2	60	12	0.30	28.2
	15.2	60	12	0.31	35.0
Mahogany Shale 100°C	15.2	100	12	0.46	40.2
	15.2	100	12	0.47	43.2
Wilcox Lignite 60°C	58	60	12	0.06	277.9
	58	60	12	0.06	280.6
Wilcox Lignite 100°C	58	100	12	0.23	342.8
	58	100	12	0.26	353.2
$NAS_{472\text{-}RD}$, 100°C	1.2	100	1	0.21	n.a.
	1.2	100	1	0.20	n.a.
$NAS_{472\text{-}RD}$, 140°C	1.2	140	1	0.93	n.a.
	1.2	140	1	0.87	n.a.
	1.2	140	1	0.91	n.a.
Yabulai Shale, 100°C	5.2	100	1	0.01	n.a.
	5.2	100	1	0.01	n.a.
Yabulai Shale, 140°C	5.2	140	1	0.02	n.a.
	5.2	140	1	0.02	n.a.

n.a., not applicable. n.d., not determined. NAS, New Albany Shale. Methane yields of NAS_{IN3}, NAS_{IN6}, Springfield Coal #2, and Second White Specks Formation were re-calculated from Ma et al. (2021), and other samples were re-calculated from Wei et al. (2018, 2019).

could be compared by simply mass balance equation. In this study, we chose to effectively compare newly catalytic gas generation yields between those two studies (Wei et al., 2018; Ma et al., 2021) with the following: the amount of catalytic generated gas equals the total amount of liberated gas yields from glass ampoules and residual gas yield in closed pores from source rock chips after heating experiments deducted yields of residual gas in closed pores of original, un-heated samples.

3.2 CH_4 and CO_2 Yields From In-Lab Simulation Heating Experiments

Wei et al. (2018) conducted low-temperature (60 and 100°C) heating experiments lasting 6 months to 1 year and provided evidence for the geo-catalytic generation of hydrocarbons from various source rocks at different hydrostatic pressures. In addition, they performed another suite of low-temperature (100 and 140°C) heating experiments from two types of source rock lasting 1 month and quantified generated CH_4 and CO_2 gas yield. Ma et al. (2021) determined the overall yield of CH_4 generated from heating experiments at 80°C, 100°C, and 120°C from source rocks of different kerogen types lasting more than 14 months. Our study re-quantified final catalytic gas generation yields using the total yield of released gas from glass ampoules and residual gas in closed pores from source rock chips after heating experiments deducting yields of residual gas in closed pores of the original, un-heated samples. Gas generation yields from those different heating experiments were re-organized and presented in **Table 3** and **Figure 2**.

The comparison shows that methane generation yields are highest from Second White Specks Formation Shale, Mowry Shale, and Springfield Coal #2 (**Figure 2**). Four NAS samples were used, covering TOC content from 1.2% to 15.1%, and their CH_4 yields were comparable. Methane yields did not express direct correlations with kerogen type, TOC content, or initial thermal maturity. Increasing heating time limitedly increased gas generation yields. For one specific source rock type, CH_4 and CO_2 yields show a certain amount of increase with increased temperature (60–120°C). For example, the CH_4 amount in Mowry Shale, Springfield Coal #1, Wilcox Lignite, Mahogany Shale, and NAS_{MM3} shows an increasing trend with elevated temperature from 60 to 100°C for 12 months. Methane yields released from Second White Specks Formation Shale, NAS_{IN3} and NAS_{IN6} also increased with heating temperature from 80°C to 100°C and 120°C.

Gas yields are expressed in μmol g^{-1} of TOC to emphasize the relation to the organic matter in source rocks (**Table 3**; **Figure 2**). In the studied shale samples, the Mowry Shale and Second White Specks Formation liberated the highest methane yields in comparison to other studied source rocks at comparable conditions, even at 60 and 80°C, but especially at 100°C over 12 and 38 months. Samples of Mahogany Shale and NAS produced small amounts of CH_4 even at 120°C over 36 months. Generally, NAS and Mahogany Shale produced comparable methane amounts at similar temperature and time conditions. Samples of NAS_{MM3} generated higher methane yields compared to Springfield #1 Coal and Wilcox Lignite at both 60°C and 100°C over 12 months. In addition, $NAS_{472\text{-}RD}$ generated methane yields of ~0.20 and ~0.90 μmol g^{-1} TOC, which is ~20 and ~45 times higher compared with methane yields from Yabulai Shale of ~0.01 and ~0.02 μmol g^{-1} TOC at 60 and

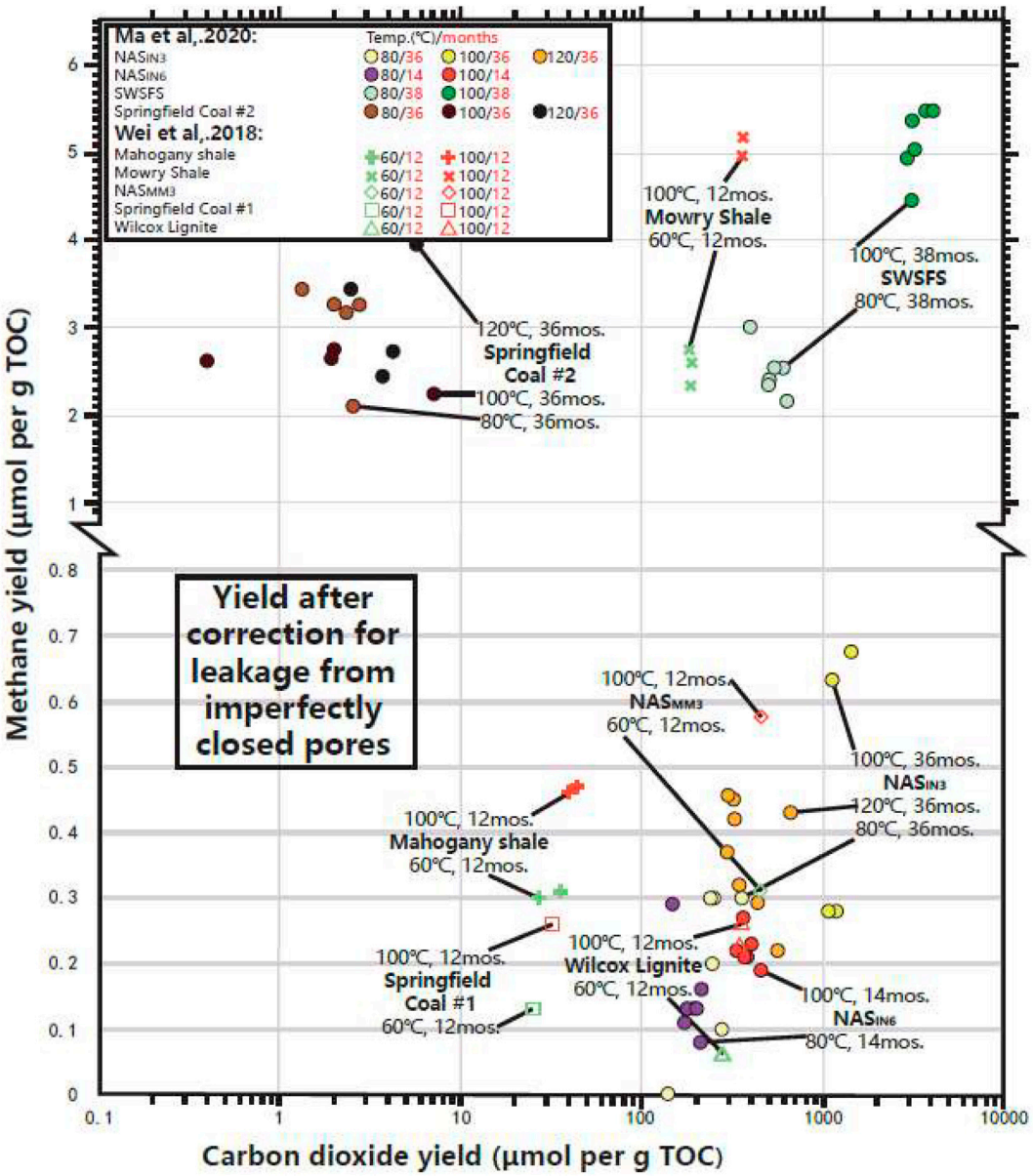

FIGURE 2 | Gas generation yields from previous heating experiments were gathered and presented. Data used in this study were re-calculated results from earlier data reported by Wei et al. (2018) and Ma et al. (2021). Final catalytic gas generation yields in this study were quantified using the total yields of released gas from glass ampoules and residual gas in closed pores from source rock chips after heating experiments deducting yields of residual gas in closed pores of original un-heated samples. The CO_2 scale is logarithmic. The reproducibility of methane and CO_2 yields was limited by the analytical uncertainty of quantification of ±0.007 µmol g^{-1} and ±0.3 µmol g^{-1}, respectively. SWSFS, Second White Specks Formation Shale.

100°C over 1 month, respectively. We also noted that Wei et al. (2018) reported CH_4 yields of only ~0.13–0.26 µmol per g TOC from Springfield Coal #1 at 100°C heating for 12 months, which is much lower than those reported for Springfield Coal #2 in Ma et al.'s (2021) study–CH_4 yields of ~2.2–2.8 µmol per g TOC after heating for 36 months at 100°C (**Figure 2**; **Table 3**). The increased heating time could not fully explain such an obvious yield difference.

Carbon dioxide is another important product liberated from the series of low-temperature heating experiments. Most coals and all shales produced much more CO_2 than CH_4. Among generated gas products, carbon dioxide (CO_2) is at a relative abundance of ~96.3–99.9 mol%, or about 30 to 10,000 times higher concentrations than all gaseous hydrocarbons combined at 100°C over 12 months of experiments. Compared to other shales, shale from the Second White Specks Formation generated large amounts of both CH_4 and CO_2 at 80 and 100°C over 38 months. Mowry and NAS generated higher amounts of CO_2 than Mahogany Shale by ~6–15 times. Results from samples of Springfield Coal #2, Springfield Coal #1, and

TABLE 4 | Organic petrography composition (volume %, on mineral matter free basis), methane yield, and related heating conditions of shale and coal samples.

Rock unit name	Alginite	AOM	Other liptinite	Solid bitumen	Vitrinite	Inertinite	Methane yield (μmol g-1 TOC)	Heating condition
Second White Specks Formation Shale	15	64	10	10	1		5.13	100°C, 38 months
$NAS_{472\text{-}RD}$	65	25	10	0	traces		1.12/ 0.21/0.90	100°C, 12 months./100°C, 1 months./140°C, 1 months
Mowry Shale	35	30	5	X	30		5.10	100°C, 12 months
Mahogany Shale	85	4	0	10	1		0.46	100°C, 12 months
Springfield Coal #1	6			X	82	12	0.26	100°C, 12 months
Springfield Coal #2	16			X	72	12	2.57	100°C, 36 months
Wilcox Lignite	8			X	82	10	0.25	100°C, 12 months
Yabulai Shale	45	5	X	10	30	10	0.01/0.02	100°C, 1 months./140°C, 1 months
NAS_{MM3}	28	19	19	33	0	1	0.58	100°C, 12 months

AOM, Amorphous organic matter. Maceral analysis results of Second White Specks Formation Shale were adopted from Furmann et al. (2015). X: not present or not counted. Heating pressures were at ambient pressure.

Mahogany Shale generated a relatively low amount of CO_2, especially in Springfield Coal #2 at 80°C, 100°C, and 120°C over 36 months. Another result worth noticing is that the CO_2 yields for NAS_{IN3} are higher at 100°C heating conditions than those at 80°C and 120°C over 36 months of experiments (**Figure 2**; **Table 3**).

3.3 Maceral Composition

Maceral compositions were analyzed and compared within studied source rocks to investigate whether there is a relationship between maceral content and CH_4 and CO_2 yields (**Table 4**). Our studied coal samples include Springfield Coal #1, Springfield #2, and Wilcox Lignite. The dominant macerals in coal samples are sporinite, vitrinite, and inertinite, but their relative proportions differ between the samples (**Table 4**). Springfield Coal #1 contains high contents of vitrinite (82 vol. %) and inertinite (12 vol. %) and a small amount of liptinite (mostly sporinite; 6 vol.%) (**Figures 3A–D**). Springfield Coal #2 has a lower content of vitrinite (72 vol. %) and inertinite (12 vol. %) and a higher amount of liptinite (mostly sporinite; 16 vol.%) (**Figures 3E,F**). Maceral in Wilcox Liginite is composed of vitrinite (82 vol. %), inertinite (10 vol. %), and a small portion of liptinite (sporinite and liptodetrinite; 8 vol. %) (**Figures 3G,H**). Similar maceral composition in Springfield Coal #1 and Wilcox Lignite indicates the limited contribution of vitrinite and inertinite to catalytic methane generation (**Table 4**). The higher liptinite content in Springfield Coal #2 obviously enhanced catalytic methane yield (**Figure 8A**).

For the shale samples, the dominant maceral group is liptinite regarded as an oil-prone maceral during thermal maturation. The macerals in studied shales are mainly composed of the liptinite group represented by alginite, AOM, and liptodetrinite, while the relative content of those varied between shale samples. The representative maceral compositions of samples from $NAS_{472\text{-}RD}$ and Yabulai Shale are shown in **Table 4**. Maceral in Yabulai Shale is composed of liptinite (mostly alginite; 69 vol. %), solid bitumen (10 vol. %), vitrinite (30 vol. %), and inertinite (10 vol. %) (**Figure 4B**). $NAS_{472\text{-}RD}$ dominantly contains liptinite (**Figure 4A**). Higher liptinite content facilitated catalytic methanogenesis in $NAS_{472\text{-}RD}$ compared to Yabulai Shale at the same heating time and temperature conditions (**Table 4**).

Liptinite in samples from the Second White Specks Formation is composed dominantly of AOM and a very low amount of well-preserved alginite (Furmann et al., 2015), in contrast to the $NAS_{472\text{-}RD}$ and Mahogany Shale where alginite (Tasmanites) is the main component. More specifically, Mowry Shale and Second White Specks Formation Shale both contain relatively high content of AOM (30% and 64%) derived from microbially degraded phytoplankton, zooplankton, and bacterial biomass, which appears structureless and occurs dispersed in the matrix or as organic streaks parallel to bedding (**Table 4**; **Figures 5A–D**). Besides AOM, Second White Specks Formation Shale and Mowry Shale contain 15% and 35% (vol. %) alginite, respectively, occurring as elongated rods perpendicular to the bedding and as flattened disks parallel to the bedding (**Figures 5B,E**). Some form discrete lenses or oval-shaped bodies with distinctive internal structures (telalginite, **Figure 5F**). The alginite shows strong greenish-yellow to yellow fluorescence under blue light irradiation. In addition, Mowry Shale contains relatively more terrestrially-derived material (vitrinite and inertinite; **Table 4** and **Figure 5A**). The CH_4 yields from NAS and Mahogany Shale are relatively lower. $NAS_{472\text{-}RD}$ and Mahogany are full of alginite, especially tasmanites occurring as discrete lenses (**Figures 6A–D**, **7**; **Table 4**); vitrinite and inertinite are rare. Alginite occurs as lamellae typically <10 μm in thickness, and cell structures are present in some occurrences (**Figures 6A,B**). $NAS_{472\text{-}RD}$ generated two times higher methane yields than NAS_{MM3} at 100°C over 12 months of heating. Maceral composition in NAS_{MM3} featured relatively averaged amounts of alginite (28 vol. %), AOM (19 vol. %), other liptinite (19 vol. %) and solid bitumen (33 vol. %), while $NAS_{472\text{-}RD}$ contained 25 vol. % of AOM and 65 vol. % of alginite. Comparing the AOM content within studied shale samples, higher AOM content in the liptinite group positively correlated with higher methane yields (**Figure 8B**).

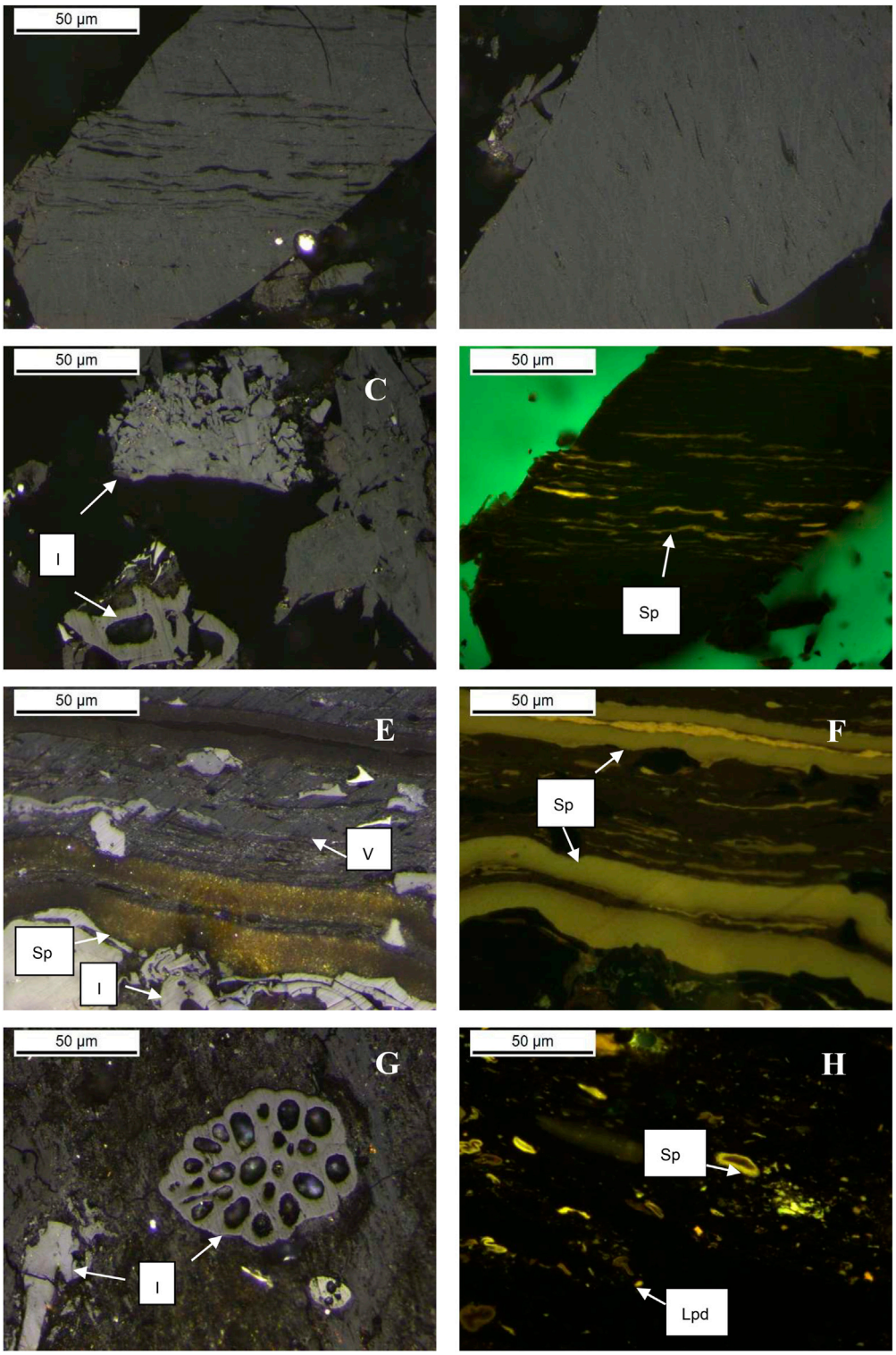

FIGURE 3 | Photomicrographs of springfield coal #1 [Panels **(A–D)**; **(A–C)**, reflected light, oil-immersion; **(D)**, fluorescent light], springfield coal #2 [Panels **(E,F)**; **(E)**, reflected light; **(F)**, fluorescent light], and Wilcox Coal [Panels **(G,H)**] under the microscope. Abbreviations: V–vitrinite, Sp–sporinite, I–inertinite, Lpd–liptodetrinite.

Organic matter is the parent material for CH_4 and CO_2 products during thermogenic gas generation. Macerals are divided into oil-prone and gas-prone, showing the quality of a source rock whether makes it more likely to generate oil or gas. Previous studies indicate the liptinite group as oil-prone maceral presents heterogeneity in the oil generation window and potential

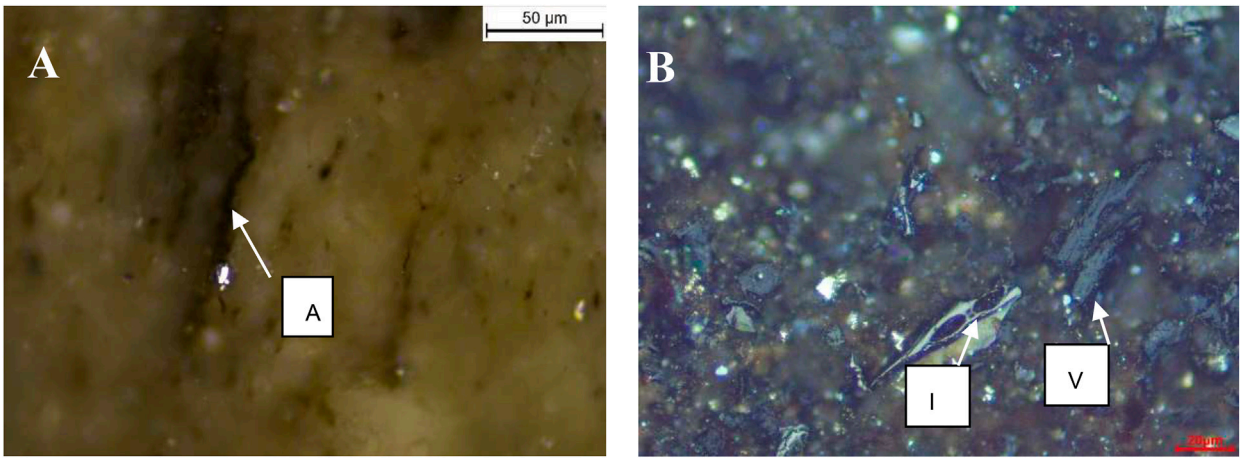

FIGURE 4 | Organic petrography photomicrographs (oil immersion, white incident light) **(A)** showing typical maceral of alginite in $NAS_{472\text{-}RD}$ **(B)** showing some vitrinite and inertinite maceral presence in Yabulai Shale. Abbreviations: V–vitrinite, A–alginite, I–inertinite.

during maturation. Resinite has the highest oil-generation potential and is usually attributed to early oil generation (R_o ~0.3–0.4%). Alginite comprises unicellular solitary or colonial algae of planktonic and benthic origin. AOM occurs as a product of variable organic matter which has undergone alteration and degradation. Liu et al. (2019a) conclude that AOM transformed to hydrocarbons earlier than alginite. Alginite derived from tasmanites cysts has higher hydrocarbon generation potential (Revill et al., 1994; Vigran et al., 2008). Cardott et al. (2015) also suggested that a post-oil solid bitumen network could have developed along with the AOM network. Vitrinite, as a gas-prone maceral, generates gas instead of oil, although most thermogenic gases are concluded from oil-cracking instead of kerogen. Hydrous pyrolysis simulation experiments (>350°C) usually indicate that the liptinite group have a higher hydrocarbon generation potential than vitrinite, including both oil and gas. Thermogenic gas generation potential from source rock is strongly controlled by kerogen type. This study further suggests that source rocks of the same kerogen type have strong heterogeneity in catalytic gas generation ability because of their specific maceral composition. Liptinite facilitates methane generation at low-temperature conditions. Moreover, alginite and AOM are the dominant liptinite maceral in marine shales, and their content can vary significantly in shales. Liu et al. (2019) proposed alginite (tasmanites in particular) is more abundant than AOM for NAS in high-energy environments. Our results proposed that AOM undergoes a transformation into gas earlier than alginite for catalytic methanogenesis, i.e., AOM is much more prone to gas than alginite in immature to marginally mature shales. Higher sporinite input also makes a positive contribution to catalytic methane generation. Vitrinite, inertinite, and solid bitumen did not show obvious differences in liberating methane gas at low temperatures.

The most dominant gas product is CO_2, which could be 30 to 10,000 times higher concentrations than hydrocarbon products in studied samples. Liptinite has a more aliphatic structure, hydrogen-rich and lower oxygen content than vitrinite (Walker and Mastalerz, 2004). Springfield Coal #2 contained more maceral liptinite than Springfield Coal #1 and generated much lower CO_2 at comparable heating temperature and longer time, which indicate that vitrinite or inertinite is easly able to liberate CO_2 upon heating than the liptinite group. In addition, higher CO_2 yields from Mowry and NAS with more terrestrial input (vitrinite, inertinite) than Mahogany Shale also proved the same point. The maceral composition can at least partly explain methane yield differences between samples. However, the related factors are still complex and need a better illustration explaining the catalytic reaction mechanism.

3.4 Reported Hydrocarbon Gas From Low-Mature Source Rock in Sedimentary Basins

Various literature reported economically viable natural gas accumulations in low-rank source rocks. What is worth noticing is that most published literature about catalytic gas were generated from humic organic matter. Galimov (1988) reported that “early thermogenic” natural gas in the Western Siberian Basin comes from humic-type organic matter. Xu et al. (2008) proposed that Jurassic coal was generated and accumulated in the gas reservoir in Turpan-Harmi Basin. Wang et al. (2005) reported immature to low mature natural gas in shallow reservoirs (<2500 m) in Liaohe and Subei Basins. Ramaswamy (2002) concluded natural gas accumulation in the North Cambay Basin in India comes from Mehsana Coal. In Qong Southeast Basin in the South China Sea, the fluid inclusion data shows (80°C–120°C) fluid inclusions providing evidence of low mature gases migrating into the reservoirs of BD 13 gas-bearing structure. The humic-type organic matters from Oligocene-Miocene source rocks (burial depth of 1570–2000 m) have a certain potential to generate biogenetic gas and low mature gas (Huang et al., 2003; Ding et al., 2018). Those reported R_o values mostly range from 0.3 to 0.5%, and reported $\delta^{13}C_{CH4}$ values are from −55‰ to −40%. Gases are

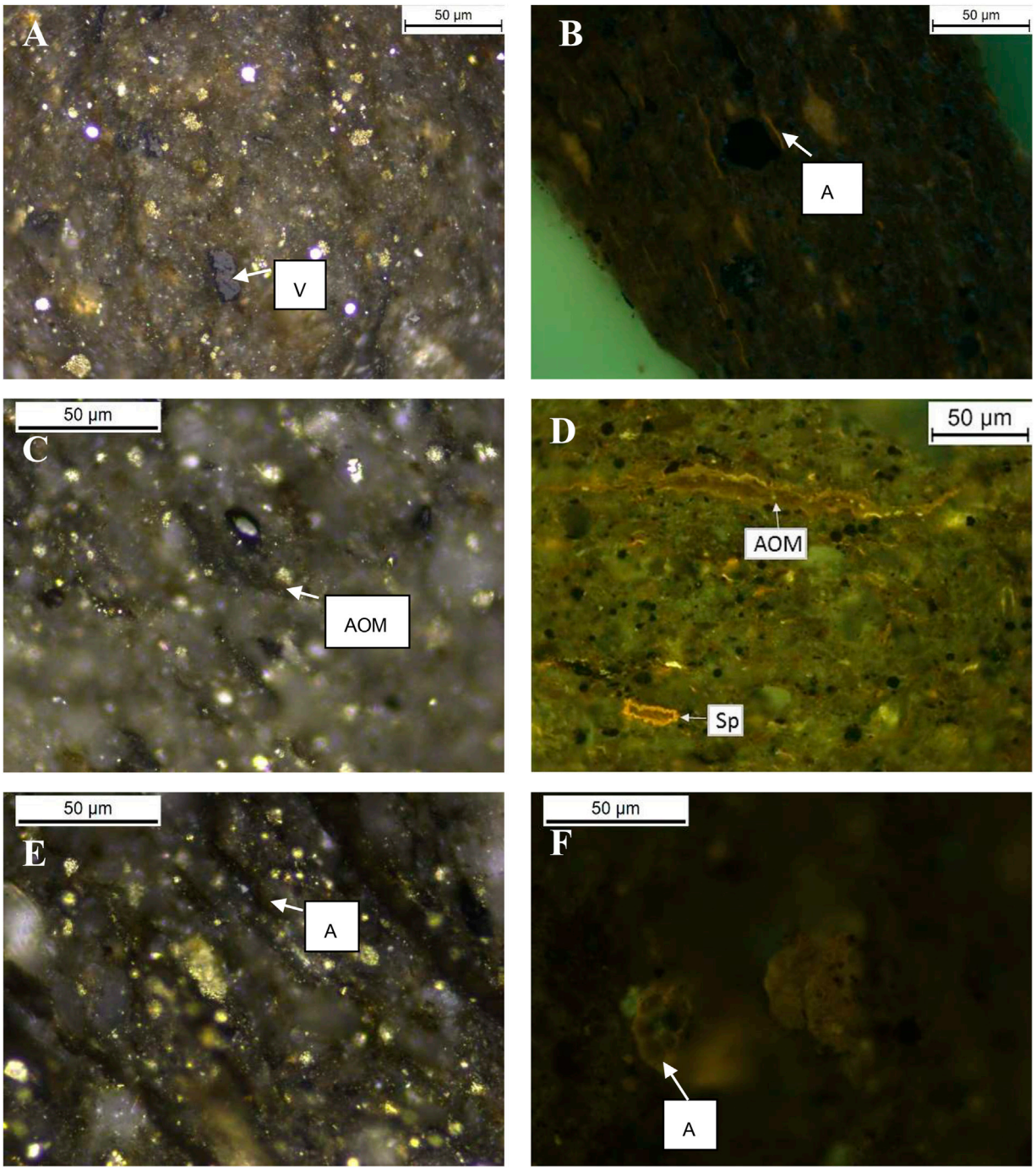

FIGURE 5 | Representative photomicrographs of macerals observed in polished blocks under reflected white and fluorescent light with an optical microscope using oil immersion. The selected pictures represent the typical type and quality of organic matter found in studied source rocks. Panels **(A,B)** were taken on samples from Mowry Shale. Most of the organic matter is composed of alginite and amorphous organic matter. Mowry also contains a certain amount of vitrinite and inertinite macerals. Panels **(C–F)** were taken on samples from Second White Specks Formation, which are mainly composed of both amorphous organic matter and alginite. Panel **(D)** was adopted from Furmann et al. (2015). Panel **(E)** shows the typical presence of Lamalginite, and Panel **(F)** shows the typical presence of Telalginite. Abbreviations: V–vitrinite, AOM–amorphous organic matter, Sp–sporinite, A–alginite, I–inertinite, Lpd–liptodetrinite.

mainly composed of CH_4 (82.48%–86.14%) with relatively high C_{2-5} components (about 10%), relatively low CO_2 (0.6%–1.2%) and N_2 (2.4%–6.7%) content, and high dry coefficients (C_1/C_{1-5} = 0.88–0.91). Fewer examples of low maturity shale strata in sedimentary basins featuring non-microbially generated hydrocarbon gas accumulations were found. For example,

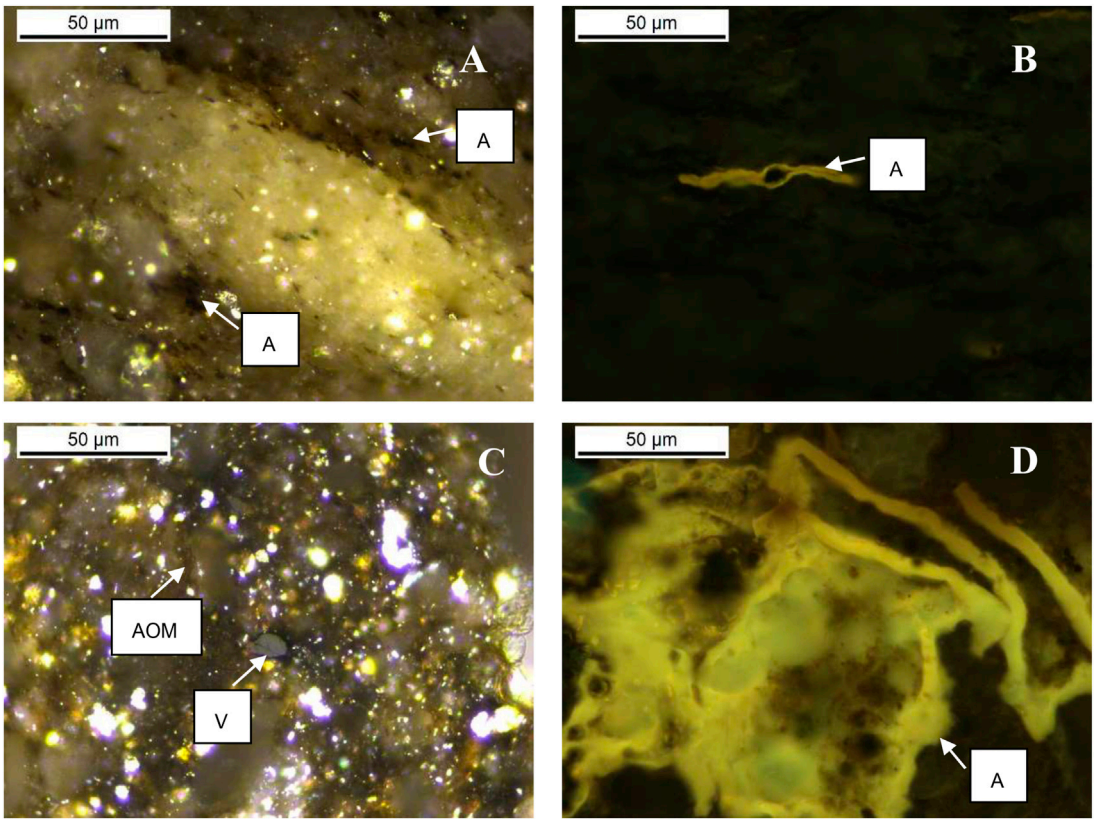

FIGURE 6 | Organic petrography photomicrographs (oil immersion, white incident light, and fluorescent light) showing typical types and morphology of organic matter in New Albany Shales. Panels **(A,B)** were taken on samples from $NAS_{472\text{-}RD}$. Panels **(C,D)** were taken on samples from NAS_{IN3} containing mainly alginite. The most representative organic matter in New Albany Shale is alginite. Abbreviations: V–vitrinite, AOM–amorphous organic matter, A–alginite.

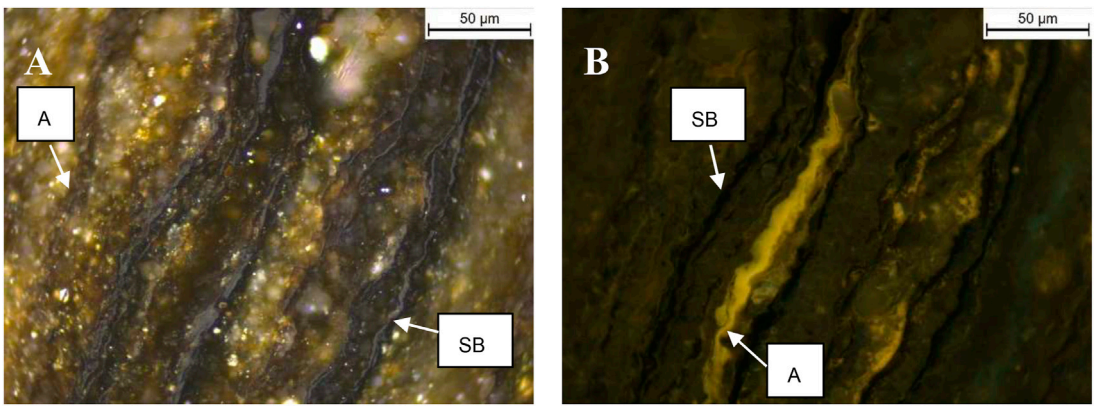

FIGURE 7 | Representative examples of photomicrographs of solid bitumen and alginite enriched Mahogany Shale [**(A)**, reflected light, oil-immersion; **(B)**, fluorescent light]. Abbreviations: SB–solid bitumen, A–alginite.

Muscio et al. (1994) proposed that immature shales released high amounts of natural gas in Williston Basin in North America with δ^{13} C_{CH4} values of ~ −33.7‰. Cardott. (2012) investigated natural gas in western Arkoma Basin in Oklahoma in America from immature Woodford Shale with δ^{13} C_{CH4} values of −52.8‰. In addition, the New Albany Shale from the Illinois basin, Mowry Shale Formation, and Second White Specks Formation in our study are mainly explored as a shale oil play in sedimentary basins (Clarkson and Pedersen, 2011). Wei et al. (2018) pointed out that considering that the New Albany Shale has been at its current

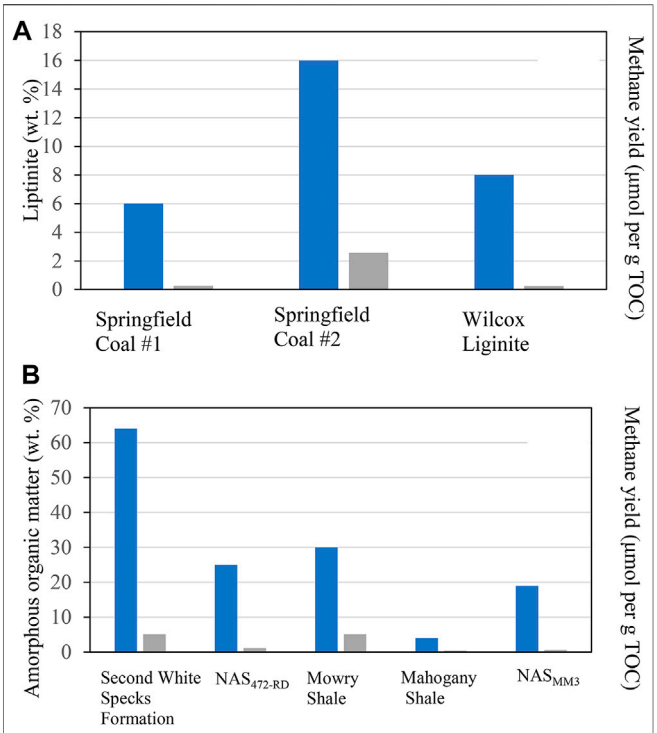

FIGURE 8 | Liptinite (wt. %, in blue) and catalytic methane generation yield (μmol per g TOC, in gray) **(A)** Amorphous organic matter (wt. %, in blue) and catalytic methane generation yield (μmol per g TOC, in gray) **(B)** of long-term heated source rock chips. The organic petrographic composition in % is on a mineral matter free basis. The presented yield data are averages of two or more independent measurements.

depth and thermal regime for approximately 90 million years (Wei et al., 2018). In this way, today's lack of abundant CH_4 in those basins testifies against significant geocatalytic methanogenesis. The reasonable explanation is that the liptinite group significantly contributes to catalytic gas generation. However, the alginite and AOM enriched shales turned to generate and expelled oil when maturity reached the oil window, while the gas-prone enriched source rock turned to continue generating thermogenic gas. Whether catalytic methanogenesis can be a significant source for natural gas accumulation is not simply related to the kerogen type of source rock but more related to the relative content of specific maceral content in shales and coals. In addition, previous studies (Wei et al., 2018) observed elevated pressures of 100 and 300 MPa caused gas yield reduction, and we proposed that lower source rock deposit with proper depth and good seal positively contributes to low-mature natural gas accumulation.

Studies on catalytic gas have indicated a high yield of 96.3–99.9 mol% carbon dioxide in gas from low-temperature heating experiments (Wei et al., 2018; Ma et al., 2021). The abundance of carbon dioxide in natural gas is highly variable yet often amounts to ~10 mol% (Lundegard and Land, 1986; Jenden et al., 1988; Smith and Ehrenberg, 1989) and much lower than in our low-temperature heating experiments. In contrast to the confined conditions in gold cells and glass tubes, the natural conditions in sedimentary basins apparently allow carbon dioxide to be removed *via* secondary processes, such as preferential dissolution in aqueous pore fluids and subsequent migration and precipitation as carbonate minerals (Ferris et al., 1994; House et al., 2006; Gilfillan et al., 2009). In addition, the long exposure to air during storage of source rocks in core lockers may have caused surficial oxygenation of organic and inorganic moieties that gave rise to CO_2 instead of methane.

3.5 Mechanism Controls on Catalytic Metagenesis

Results of metal concentration analysis are available in **Table 5**. Typical variations of sensitive trace metals in $NAS_{472\text{-}RD}$, NAS_{MM3}, and Mowry Shale, including Cr, Fe, Ni, Cu, Zn, Cd, Ba, and Pb, are presented. Methane yields differences between studied shale samples did not exhibit obvious relationships with trace metal concentration. Considering the proposed hypotheses for catalytic gas generation, the reduced metallic catalyst content lacking a relationship with methane yields in studied samples thus denied their contribution to aiding catalytic methanogenesis. Both coals used have comparable sulfur contents (~4 wt.%), thus the difference in gas yields cannot be explained by sulfur-induced lower activation energy for hydrocarbon generation in one coal compared to the other (Ma et al., 2021). In addition, certain types of macerals undergo easier and earlier bond breaking to generate light hydrocarbons. Rahman et al. (2018) conducted a study on source fabric's influence on clay mineral catalysis as it controls the extent to which organic matter and clay minerals are physically associated. They used 1) a particulate fabric where organic matter (alginite) is present as discrete (>5 μm; sample from the Permian Stuart Range Formation) and 2) a nanocomposite fabric in which AOM is associated with clay mineral surfaces at the sub-micron scale (sample from the Miocene Monterey Formation). Kinetic experiments are performed on paired whole rock and kerogen isolate samples from these two formations. More specifically, no significant difference in the modelled hydrocarbon generation window of paired whole rock and kerogen isolates from the Stuart Range Formation. Extrapolation to a modelled geological heating rate shows a 20°C reduction in the onset temperature of hydrocarbon generation in the Monterey Formation whole-rock samples relative to paired kerogen isolates. The extent to which organic matter and clay minerals are physically associated could have a significant effect on the timing of hydrocarbon generation (Rahman et al., 2018). Following their proposed idea, we also considered the organic matter and clay minerals contact extent in our samples, especially shale samples composed mainly of the liptinite group. Kus et al. (2017) concluded several identification rules distinguishing the AOM and alginite. Alginite presents the optically identifiable and recognizable lamellar structure, and isolated forms clearly distinguishable from one another and from the mineral groundmass. In comparison, the AOM, generally considered to be a degradation product, usually presents thin, small lenses and irregular stripers, porous, was also observed to occur in groundmass having close contact with clay minerals (Taylor et al., 1998). Although liptinite expresses a higher potential for

TABLE 5 | Shale metal concentrations with values reported in percentage and PPM.

Sample name	Cr	Fe	Ni	Cu	Zn	Cd	Ba	Pb
	ppm in sample	% in sample	ppm in sample	ppm in sample	ppm in sample	ppm in sample	ppm in sample	ppm in sample
$NAS_{472\text{-}RD}$	81.8	3.4	73	59.9	132.6	0.7	403.5	29.2
NAS_{MM3}	76.5	6.3	139.5	84.1	85.4	0.6	330.6	21.4
Mowry Shale	40.2	1.9	34.6	34.6	126.3	1.5	332.1	15.2

methanogenesis, the differences between AOM and alginite generating catalytic gas could also be related to their contact area with surrounding minerals. New Albany Shale and Mahogany Shale generating lower hydrocarbon gas are characterized as relatively large, discrete organic particles of alginite (tasmanites in particular) and solid bitumen having limited contact with the mineral matrix and the clay mineral. In comparison, Mowry and Second White Specks Formation Shale with higher AOM debris content associated with clay mineral surface intimately which lower its catalytic reaction. However, further quantitative evidence of OM and clay mineral contact area is needed before reaching a solid mechanism explanation.

4 CONCLUSION

This study contributed to gathering experimental evidence that catalytic methanogenesis happens at temperatures from 60 to 140°C from a variety of immature to early-mature source rocks from laboratory and further investigated maceral composition influence on methane and carbon dioxide yields catalytically generated in laboratory and sedimentary basins.

Pre-existing gas in closed pores in rock chips could mimic the amount of newly generated gas after in-lab heating simulation experiment. The amount of geo-catalytically generated CH_4 and CO_2 during long-term heating experiments was obtained by using the total yields of released gas from glass ampoules and residual gas in closed pores from source rock chips after heating experiments deducting yields of residual gas in closed pores of the original un-heated samples.

Different shales and coals express various yields of catalytically generated CH_4 and CO_2 upon low-temperature heating from 60°C to 140°C. The reduced metallic catalyst content lacking a relationship with methane yields in the studied samples thus denied their contribution to aiding catalytic methanogenesis. Both coals used have comparable sulfur contents, and thus the difference in gas yields cannot be explained by sulfur-induced lower activation energy for hydrocarbon generation in one coal compared to the other. Higher temperatures and increased heating time can enhance the activity of geo-catalytic methanogenesis. Organic petrographic evidence from two types of Springfield Coals with comparable thermal maturity suggests that liptinite expresses a far higher potential for methanogenesis but liberates less CO_2 than vitrinite. The CH_4 yields of the Mowry Shale and Second White Specks Formation are approximately ten times higher than those of the Mahogany Shale and New Albany Shale, further suggesting that the AOM express better ability than telalginite in catalytic methane generation. Higher sporinite input also makes a positive contribution to catalytic methane generation. Vitrinite, inertinite, and solid bitumen did not show obvious differences in liberating methane gas at low temperatures.

DATA AVAILABILITY STATEMENT

The original contributions presented in the study are included in the article/Supplementary Material, further inquiries can be directed to the corresponding authors.

AUTHOR CONTRIBUTIONS

LW contributed to manuscript organizing and writing. KZ and XC contributed to data editing and revising. JY, JL, and CL contributed to the figure and table revising.

FUNDING

This work was supported by the Fundamental Research Funds for China University of Geosciences (Beijing) under Award Numbers 35832019035 and 53200759769. Financial support from the National Natural Science Foundation of China under Award Number 41702133 is also greatly appreciated.

REFERENCES

Baskin, D. K., and Peters, K. E. (1992). Early Generation Characteristics of a Sulfur-Rich Monterey Kerogen. *AAPG Bull.* 76, 1–13. doi:10.1306/bdff874a-1718-11d7-8645000102c1865d

Bu, H., Yuan, P., Liu, H., Liu, D., Liu, J., He, H., et al. (2017). Effects of Complexation between Organic Matter (OM) and clay mineral on OM Pyrolysis. *Geochimica et Cosmochimica Acta* 212, 1–15. doi:10.1016/j.gca.2017.04.045

Cardott, B. J. (2012). Thermal Maturity of Woodford Shale Gas and Oil Plays, Oklahoma, USA. *Int. J. Coal Geology.* 103, 109–119. doi:10.1016/j.coal.2012.06.004

Cardott, B. J., Landis, C. R., and Curtis, M. E. (2015). Post-Oil Solid Bitumen Network in the Woodford Shale, USA-A Potential Primary Migration Pathway. *Int. J. Coal Geol.* 139, 106–113.

Carothers, W. W., and Kharaka, Y. K. (1978). Aliphatic Acid Anions in Oil fields Waters–Implication for the Origin of Natural Gas. *AAPG Bull.* 62, 2441–2453. doi:10.1306/c1ea5521-16c9-11d7-8645000102c1865d

Clarkson, C. R., and Pedersen, P. K. (2011). "Production Analysis of Western Canadian Unconventional Light Oil Plays," in Society Of Petroleum Engineers. Canadian Unconventional Resources Conference (Calgary, Alberta: Canada), 23. doi:10.2118/149005-ms

Ding, W., Hou, D., Zhang, W., He, D., and Cheng, X. (2018). A New Genetic Type of Natural Gases and Origin Analysis in Northern Songnan-Baodao Sag, Qiongdongnan Basin, South China Sea. *J. Nat. Gas Sci. Eng.* 50, 384–398. doi:10.1016/j.jngse.2017.12.003

Espitalié, J., Makadi, K. S., and Trichet, J. (1984). Role of mineral Matrix during Kerogen. *Pyrolysis. Org. Geochem.* 6, 365–382.

Ferris, F. G., Wiese, R. G., and Fyfe, W. S. (1994). Precipitation of Carbonate Minerals by Microorganisms: Implications for Silicate Weathering and the Global Carbon Dioxide Budget. *Geomicrobiology J.* 12 (1), 1–13. doi:10.1080/01490459409377966

Furmann, A., Mastalerz, M., Brassell, S. C., Pedersen, P. K., Zajac, N. A., and Schimmelmann, A. (2015). Organic Matter Geochemistry and Petrography of Late Cretaceous (Cenomanian-Turonian) Organic-Rich Shales from the Belle Fourche and Second White Specks Formations, West-central Alberta, Canada. *Org. Geochem.* 85, 102–120. doi:10.1016/j.orggeochem.2015.05.002

Galimov, E. M. (1988). Sources and Mechanisms of Formation of Gaseous Hydrocarbons in Sedimentary Rocks. *Chem. Geology.* 71, 77–95. doi:10.1016/0009-2541(88)90107-6

Gao, L., Schimmelmann, A., Tang, Y., and Mastalerz, M. (2014). Isotope Rollover in Shale Gas Observed in Laboratory Pyrolysis Experiments: Insight to the Role of Water in Thermogenesis of Mature Gas. *Org. Geochem.* 68, 95–106. doi:10.1016/j.orggeochem.2014.01.010

Hackley, P. C., and Cardott, B. J. (2016). Application of Organic Petrography in North American Shale Petroleum Systems: A Review. *Int. J. Coal Geol.* 163, 8. doi:10.1016/j.coal.2016.06.010

Higgs, M. D. (1986). "Laboratory Studies into the Generation of Natural Gas from Coals,". Editors N. W. Europe and J. Brooks (London: Geol. Soc. Lond. Spec. Publ.), 23, 113–120. doi:10.1144/gsl.sp.1986.023.01.08

House, K. Z., Schrag, D. P., Harvey, C. F., and Lackner, K. S. (2006). Permanent Carbon Dioxide Storage in Deep-Sea Sediments. *Proc. Natl. Acad. Sci. U.S.A.* 103, 12291–12295. doi:10.1073/pnas.0605318103

Huang, B., Xiao, X., and Li, X. (2003). Geochemistry and Origins of Natural Gases in the Yinggehai and Qiongdongnan Basins, Offshore South China Sea. *Org. Geochem.* 34 (7), 1009–1025. doi:10.1016/s0146-6380(03)00036-6

Hunt, J. M. (1996). *Petroleum Geochemistry and Geology*. New York: W. H. Freeman, 743.

ICCP, International Committee for Coal Petrology (2001). The New Inertinite Classification (ICCP System 1994). *Fuel* 80, 459. doi:10.1016/S0016-2361(00)00102-2

ICCP, International Committee for Coal Petrology (1998). The New Vitrinite Classification (ICCP System 1994). *Fuel* 77, 349. doi:10.1016/S0016-2361(98)80024-0

Inagaki, F., Hinrichs, K.-U., Kubo, Y., Bowles, M. W., Heuer, V. B., Hong, W.-L., et al. (2015). Exploring Deep Microbial Life in Coal-Bearing Sediment Down to ~2.5 Km below the Ocean Floor. *Science* 349 (6246), 420–424. doi:10.1126/science.aaa6882

Jadoon, Q. K., Roberts, E., Blenkinsop, T., and Wust, R. (2016). Organic Petrography and thermal Maturity of the Permian Roseneath and Murteree Shales in the Cooper Basin, Australia. *Int. J. Coal Geology.* 154-155, 240–256. doi:10.1016/j.coal.2016.01.005

Jarvie, D. M., Hill, R. J., Ruble, T. E., and Pollastro, R. M. (2007). Unconventional Shale-Gas Systems: The Mississippian Barnett Shale of north-central Texas as One Model for Thermogenic Shale-Gas Assessment. *Bulletin* 91 (4), 475–499. doi:10.1306/12190606068

Jenden, P. D., Kaplan, I. R., Poreda, R., and Craig, H. (1988). Origin of Nitrogen-Rich Natural Gases in the California Great Valley: Evidence from Helium, Carbon and Nitrogen Isotope Ratios. *Geochimica et Cosmochimica Acta* 52, 851–861. doi:10.1016/0016-7037(88)90356-0

Jin, H., Schimmelmann, A., Mastalerz, M., Pope, J., and Moore, T. A. (2010). Coalbed Gas Desorption in Canisters: Consumption of Trapped Atmospheric Oxygen and Implications for Measured Gas Quality. *Int. J. Coal Geology.* 81 (1), 64–72. doi:10.1016/j.coal.2009.10.010

Kendall, B., Creaser, R. A., Gordon, G. W., and Anbar, A. D. (2009). Re-Os and Mo Isotope Systematics of Black Shales from the Middle Proterozoic Velkerri and Wollogorang Formations, McArthur Basin, Northern Australia. *Geochim. Cosmochim. Acta.* 73 (9), 2534–2558

Khavari Khorasani, G., and Michelsen, J. K. (1991). Geological and Laboratory Evidence for Early Generation of Large Amounts of Liquid Hydrocarbons from Suberinite and Subereous Components. *Org. Geochem.* 17 (6), 849–863. doi:10.1016/0146-6380(91)90025-f

Khorasani, G., and Murchison, D. (1988). Order of Generation of Petroleum Hydrocarbons from Liptinic Macerals with Increasing thermal Maturity. *Fuel* 67 (8), 1160–1162. doi:10.1016/0016-2361(88)90388-2

Kotarba, M. J., and Lewan, M. D. (2004). Characterizing Thermogenic Coalbed Gas from Polish Coals of Different Ranks by Hydrous Pyrolysis. *Org. Geochem.* 35, 615–646. doi:10.1016/j.orggeochem.2003.12.001

Kus, J., Araujo, C. V., Borrego, A. G., Flores, D., Hackley, P. C., Hámor-Vidó, M., et al. (2017). Identification of Alginite and Bituminite in Rocks Other Than Coal. 2006, 2009, and 2011 Round Robin Exercises of the ICCP Identification of Dispersed Organic Matter Working Group. *Int. J. Coal Geol.* 178, 26–38.

Lewan, M. D. (1991). Generation and Expulsion of Oil as Determined by Hydrous Pyrolysis. *AAPG Bull.* 75, 620. doi:10.1306/0c9b0553-1710-11d7-8645000102c1865d

Lewan, M. D., and Kotarba, M. J. (2014). Thermal-maturity Limit for Primary Thermogenic-Gas Generation from Humic Coals as Determined by Hydrous Pyrolysis. *Bulletin* 98 (12), 2581–2610. doi:10.1306/06021413204

Lewan, M. D., Kotarba, M. J., Więcław, D., and Piestrzyński, A. (2008). Evaluating Transition-Metal Catalysis in Gas Generation from the Permian Kupferschiefer by Hydrous Pyrolysis. *Geochimica et Cosmochimica Acta* 72 (16), 4069–4093. doi:10.1016/j.gca.2008.06.003

Lewan, M. D. (1998). Sulphur-radical Control on Petroleum Formation Rates. *Nature* 391, 164–166. doi:10.1038/34391

Lin, R., and Patrick Ritz, G. (1993). Studying Individual Macerals Using i.R. Microspectrometry, and Implications on Oil versus Gas/condensate Proneness and "Low-Rank" Generation. *Org. Geochem.* 20 (6), 695–706. doi:10.1016/0146-6380(93)90055-g

Liu, B., Mastalerz, M., Schieber, J., and Teng, J. (2020). Association of Uranium with Macerals in marine Black Shales: Insights from the Upper Devonian New Albany Shale, Illinois Basin. *Int. J. Coal Geology.* 217, 103351. doi:10.1016/j.coal.2019.103351

Liu, B., Schieber, J., and Mastalerz, M. (2017). Combined SEM and Reflected Light Petrography of Organic Matter in the New Albany Shale (Devonian-Mississippian) in the Illinois Basin: A Perspective on Organic Pore Development with thermal Maturation. *Int. J. Coal Geology.* 184, 57–72. doi:10.1016/j.coal.2017.11.002

Liu, B., Schieber, J., and Mastalerz, M. (2019a). "Petrographic and Micro-FTIR Study of Organic Matter in the Upper Devonian New Albany Shale during Thermal Maturation: Implications for Kerogen Transformation,". Editors W. Camp, K. Milliken, K. Taylor, N. Fishman, P. Hackley, and J. Macquaker (AAPG Mem), 120, 165–188. doi:10.1306/13672216m1213380*Mudstone Diagenesis: Res. Perspect. Shale Hydrocarbon Reservoirs, Seals, Source Rocks*

Liu, B., Schieber, J., Mastalerz, M., and Teng, J. (2019b). Organic Matter Content and Type Variation in the Sequence Stratigraphic Context of the Upper Devonian New Albany Shale, Illinois Basin. *Sediment. Geol.* 383, 101. doi:10.1016/j.sedgeo.2019.02.004

Lundegard, P. D., and Land, L. S. (1986). "Carbon Dioxide and Organic Acids: Their Role in Porosity Enhancement and Cementation, Paleogene of the Texas Gulf Coast," in *Roles of Organic Matter in Sediment Diagenesis*. Editor D. L. Gautier (Colorado: Soc. Econ. Pal. Mineral. Spec. Publ.), 38, 129–146. doi:10.2110/pec.86.38.0129

Ma, X., Liu, B., Brazell, C., Mastalerz, M., Drobniak, A., and Schimmelmann, A. (2021). Methane Generation from Low-Maturity Coals and Shale Source Rocks at Low Temperatures (80-120 °C) over 14-38 Months. *Org. Geochem.* 155, 104224. doi:10.1016/j.orggeochem.2021.104224

Mango, F. D., and Jarvie, D. M. (2009). Low-temperature Gas from marine Shales: Wet Gas to Dry Gas over Experimental Time. *Geochem. Trans.* 10 (1), 10–11. doi:10.1186/1467-4866-10-10

Mango, F. D. (1996). Transition Metal Catalysis in the Generation of Natural Gas. *Org. Geochem.* 24 (10), 977–984. doi:10.1016/s0146-6380(96)00092-7

Mango, F. D. (1992). Transition Metal Catalysis in the Generation of Petroleum and Natural Gas. *Geochim. Cosmochim. Acta* 56, 553

Martini, A. M., Walter, L. M., and McIntosh, J. C. (2008). Identification of Microbial and Thermogenic Gas Components from Upper Devonian Black Shale Cores, Illinois and Michigan Basins. *Bulletin* 92 (3), 327–339. doi:10.1306/10180706037

Mastalerz, M., Drobniak, A., and Stankiewicz, A. B. (2018). Origin, Properties, and Implications of Solid Bitumen in Source-Rock Reservoirs: a Review. *Int. J. Coal Geology.* 195, 14–36. doi:10.1016/j.coal.2018.05.013

Mastalerz, M., Schimmelmann, A., Lis, G. P., Drobniak, A., and Stankiewicz, A. (2012). Influence of Maceral Composition on Geochemical Characteristics of Immature Shale Kerogen: Insight from Density Fraction Analysisfluence of Maceral Composition on Geochemical Characteristics of Immature Shale Kerogen: Insight from Density Fraction Analysis. *Int. J. Coal Geology.* 103, 60–69. doi:10.1016/j.coal.2012.07.011

Medina, J. C., Butala, S. J., Bartholomew, C. H., and Lee, M. L. (2000). Low Temperature Iron- and Nickel-Catalyzed Reactions Leading to Coalbed Gas Formation. *Geochimica et Cosmochimica Acta* 64 (4), 643–649. doi:10.1016/s0016-7037(99)00348-8

Milkov, A. V., and Etiope, G. (2018). Revised Genetic Diagrams for Natural Gases Based on a Global Dataset of >20,000 Samples. *Org. Geochem.* 125, 109–120. doi:10.1016/j.orggeochem.2018.09.002

Muscio, G. P. A., Horsfield, B., and Welte, D. H. (1994). Occurrence of Thermogenic Gas in the Immature zone–Implications from the Bakken In-Source Reservoir System. *Org. Geochem.* 22 (3), 461–476. doi:10.1016/0146-6380(94)90119-8

Orr, W. L. (1983). "Comments on Pyrolytic Hydrocarbon Yields in Source-Rock Evaluations," in *Advances in Organic Geochemistry 1981*. Editor M. Bjorøy (New York: Wiley), 775–787.

Paull, C. K., Lorenson, T. D., Borowski, W. S., Ussler, W., III., Olsen, K., and Rodriguez, N. M. (2000). "Isotopic Composition of CH_4, CO_2 Species, and Sedimentary Organic Matter within Samples from the Blake Ridge: Gas Source Implications," in *Proc. Ocean Drilling Program Scientific Results*. Editor C. K. Paull 164, 67–78. http://www-odp.tamu.edu/Publications/164_SR/VOLUME/CHAPTERS/SR164_07.PDF.

Peters, K. E., Walters, C. C., and Mankiewicz, P. J. (2006). Evaluation of Kinetic Uncertainty in Numerical Models of Petroleum Generation. *Bulletin* 90, 387–403. doi:10.1306/10140505122

Petersen, H. I., Bojesen-Koefoed, J. A., and Mathiesen, A. (2010). Variations in Composition, Petroleum Potential and Kinetics of Ordovician-Miocene Type I and Type I-II Source Rocks (Oil Shales): Implications for Hydrocarbon Generation Characteristics. *J. Petrol. Geol.* 33 (1), 19–41.

Pickel, W., Kus, J., Flores, D., Kalaitzidis, S., Christanis, K., Cardott, B. J., et al.ICCP (2017). Classification of Liptinite - ICCP System 1994fication of Liptinite–ICCP System 1994. *Int. J. Coal Geology.* 169, 40–61. doi:10.1016/j.coal.2016.11.004

Rahman, H. M., Kennedy, M., Löhr, S., Dewhurst, D. N., Sherwood, N., Yang, S., et al. (2018). The Influence of Shale Depositional Fabric on the Kinetics of Hydrocarbon Generation through Control of mineral Surface Contact Area on clay Catalysisfluence of Shale Depositional Fabric on the Kinetics of Hydrocarbon Generation through Control of mineral Surface Contact Area on clay Catalysis. *Geochimica et Cosmochimica Acta* 220, 429–448.doi:10.1016/j.gca.2017.10.012

Ramaswamy, G. (2002). A Field Evidence for mineral-catalyzed Formation of Gas during Coal Maturation. *Oil Gas J.* 100, 32–36.

Rice, D. D., and Claypool, G. E. (1981). Generation, Accumulation, and Resource Potential of Biogenic Gas. *AAPG Bull.* 65 (1), 5–25. doi:10.1306/2f919765-16ce-11d7-8645000102c1865d

Rowe, D., and Muehlenbachs, A. (1999). Low-temperature thermal Generation of Hydrocarbon Gases in Shallow Shales. *Nature* 398 (6722), 61–63. doi:10.1038/18007

Savage, P. E. (2000). Mechanisms and Kinetics Models for Hydrocarbon Pyrolysis. *J. Anal. Appl. Pyrolysis* 54, 109–126. doi:10.1016/s0165-2370(99)00084-4

Seewald, J. S. (2003). Organic-inorganic Interactions in Petroleum-Producing Sedimentary Basins. *Nature* 426, 327

Smith, J. T., and Ehrenberg, S. N. (1989). Correlation of Carbon Dioxide Abundance with Temperature in Clastic Hydrocarbon Reservoirs: Relationship to Inorganic Chemical Equilibrium. *Mar. Pet. Geology.* 6, 129–135. doi:10.1016/0264-8172(89)90016-0

Smyth, M. (1983). Nature of Source Material for Hydrocarbons in Cooper Basin, Australia. *AAPG Bull.* 67 (9), 1422–1426. doi:10.1306/03b5ba42-16d1-11d7-8645000102c1865d

Snowdon, L. R. (1991). Oil from Type III Organic Matter: Resinite Revisited. *Org. Geochem.* 17 (6), 743–747. doi:10.1016/0146-6380(91)90018-f

Stainforth, J. G. (2009). Practical Kinetic Modeling of Petroleum Generation and Expulsion. *Mar. Pet. Geology.* 26 (4), 552–572. doi:10.1016/j.marpetgeo.2009.01.006

Stasiuk, L. D. (1994). Fluorescence Properties of Palaeozoic Oil-Prone Alginite in Relation to Hydrocarbon Generation, Williston Basin, Saskatchewan, Canada. *Mar Pet Geol.* 11 (2), 219–231.

Taylor, G. H., Teichmüller, M., Davis, A., Diessel, C. F. K., Littke, R., and Robert, P. (1998). *Organic Petrology*. Stuttgart, Berlin: Gebrüder Borntraeger, 704.

Tilley, B., and Muehlenbachs, K. (2006). Gas Maturity and Alteration Systematics across the Western Canada Sedimentary Basin from Four Mud Gas Isotope Depth Profilesiles. *Org. Geochem.* 37, 1857–1868. doi:10.1016/j.orggeochem.2006.08.010

Tissot, B. P., and Welte, D. H. (1984). *Petroleum Formation and Occurrence*. Berlin: Springer-Verlag, 699.

Walker, R., and Mastalerz, M. (2004). Functional Group and Individual Maceral Chemistry of High Volatile Bituminous Coals from Southern Indiana: Controls on Coking. *Int. J. Coal Geology.* 58, 181–191. doi:10.1016/j.coal.2003.10.008

Wang, W., Liu, W., Xu, Y., Shen, P., Kang, Y., and Ren, J. (2005). Genetic Identification of Natural Gases from Shallow Reservoirs in Some Oil- and Gas-Bearing Basins of China. *Chin. J. Geochem.* 24 (1), 90–94.

Wei, L., Gao, Z., Mastalerz, M., Schimmelmann, A., Gao, L., Wang, X., et al. (2019). Influence of Water Hydrogen on the Hydrogen Stable Isotope Ratio of Methane at Low versus High Temperatures of Methanogenesis. *Org. Geochem.* 128, 137–147. doi:10.1016/j.orggeochem.2018.12.004

Wei, L., Schimmelmann, A., Mastalerz, M., Lahann, R. W., Sauer, P. E., Drobniak, A., et al. (2018). Catalytic Generation of Methane at 60-100 °C and 0.1-300 MPa from Source Rocks Containing Kerogen Types I, II, and III. *Geochimica et Cosmochimica Acta* 231, 88–116. doi:10.1016/j.gca.2018.04.012

Wei, L., Sun, S., Dong, D., Shi, Z., Yin, J., Zhang, S., et al. (2021). *Petrographic Characterization and Maceral Controls on Porosity in Overmature marine Shales: Examples from Ordovician-Silurian Shales in China and.* U.S. Geofluids, 5582262

Wei, L., Wang, Y., and Mastalerz, M. (2016). Comparative Optical Properties of Macerals and Statistical Evaluation of Mis-Identification of Vitrinite and Solid Bitumen from Early Mature Middle Devonian - Lower Mississippian New Albany Shale: Implications for thermal Maturity Assessment. *Int. J. Coal Geology.* 168, 222–236. doi:10.1016/j.coal.2016.11.003

Whiticar, M. J. (1999). Carbon and Hydrogen Isotope Systematics of Bacterial Formation and Oxidation of Methane. *Chem. Geol.* 161 (1), 291–314. doi:10.1016/s0009-2541(99)00092-3

Xu, Y., Wang, Z., Wang, X., Zheng, J., and Du, H. (2008). Low-mature Gases and Typical Low-Mature Gas fields in China. *Sci. China Ser. D-earth Sci.* 51 (2), 312–320. doi:10.1007/s11430-008-0011-x

Yang, J., Hatcherian, J., Hackley, P. C., and Pomerantz, A. E. (2017). Nanoscale Geochemical and Geomechanical Characterization of Organic Matter in Shale. *Nat. Commun.* 8, 2179. doi:10.1038/s41467-017-02254-0

Conflict of Interest: The authors declare that the research was conducted in the absence of any commercial or financial relationships that could be construed as a potential conflict of interest.

Publisher's Note: All claims expressed in this article are solely those of the authors and do not necessarily represent those of their affiliated organizations, or those of the publisher, the editors, and the reviewers. Any product that may be evaluated in this article, or claim that may be made by its manufacturer, is not guaranteed or endorsed by the publisher.